The Effect of Cooling Rate on the Solutionizing of IN718 Superalloy Produced via Selective Laser Melting (SLM) Method

H. H. Dastgerdi[1], M. O. Shabani[2,3], Y. Shajari[2,*]

[1]*Iran University of Industries and Mines (IUIM), Tehran, Iran.*
[2]*Institute of Materials and Energy, Meshkin Dasht, Karaj, Iran.*
[3]*Department of Mining and Metallurgical Engineering, Amirkabir University of Technology, Tehran, Iran.*
Received: 05 September 2018 - Accepted: 13 January 2019

Abstract

In the present study, IN718 super alloy was produced by selective laser melting (SLM) method and was imposed under solution heat treatment at temperature of 1040°C for 2 hours. Three different environments, such as water, air and furnaces were used to cool the samples after complete solution. The results of microstructural studies conducted by optical microscopy (OM) and field emission scanning electron microscopy (FESEM) showed that intermetallic precipitates were formed during the process, disappear after solution. In order to complete the FESEM results, X-Ray diffraction (XRD) test showed that in at all cooling rates, the only remaining phases of matrix are the austenite (γ) and carbides, which their locations are between the grains according to the microscopic images. This issue indicates the proper selection of solution parameters and proper execution of solution process. The micro hardness test showed that doing solution treatment to reduce the volume fraction or completely remove the secondary phase leads to decreased hardness. By increasing cooling rate, the hardness of samples was reduced, so that the hardness of sample chilled in 30 % water was reduced compared to the sample before the heat treatment.

Keywords: IN718 Superalloy, Selective Laser Melting (SLM), Solution Heat Treatment, Microstructure, Hardness.

1. Introduction

Gas power plants play a significant role to supply the required power and energy of a country, improve the performance of each component of these plants that ultimately leads to increase the efficiency and reduced operating costs. Gas turbines are one of the most basic devices used in these plants. Gas turbines are used as driving engine for airplanes, fighter jets, ships and trains. More than half of the gas turbine parts are made of nickel-based super alloys. Improving the mechanical and chemical properties of different parts of the gas turbine will ultimately increase their durability and turbine efficiency [1]. Engineering properties, especially the mechanical behavior of nickel-bases super alloys, are heavily influenced by the primary and secondary processes of their production [2]. One of the most applied superalloys in gas turbine parts (blades, discs and shafts) is IN718 super alloy. IN718 super alloy is commonly used in embedded form. Perhaps in some turbines, casting parts can be found from this alloy. One of the methods of manufacturing gas turbine parts recently considered to be significant is Additive Manufacturing (AM) [1,3]. An additive manufacturing (AM) is a generic name that is used for manufacturing methods that enable the production of components directly from a 3D environment of computer data design by adding layer to layer materials until the final component is obtained.

Unlike the conventional manufacturing methods, in which a component is made of a block with considered materials by machine, in AM, the required materials are selectively added. By doing this, pure components with low waste materials can be produced, while conventional production methods generate a lot of waste. Over the past decade, AM has attracted much attention as a background to research, especially in the aerospace, nuclear and automotive industries [4]. Selective laser melting (SLM) is a layer to layer additive production method that uses a high-intensity laser beam to melt a desired volume in a powder room. The powder is spread on a bed using a distribution mechanism in a thin layer (with thickness of few tenths of a micro meter). The laser beam scans and melts powder and forms the first layer of manufacturing. The next layer is consecutively made by placing the building platform from a building layer to place the next layer of powder above the first layer. [5]. A pocket with inert gas is manufactured to protect materials from oxygen and nitrogen that can be created during warming of unwanted reactions in materials, such as oxide and nitride formation. Another benefit is the possibility of using low pressure or vacuum environment to protect the warm material [6].

The thermal process of nickel-based super alloys is generally to solidify through the sedimentation or retrieval of its engineering properties. In previous

*Corresponding author
Email address: y.shajari@merc.ac.ir

studies, it has been shown that in sedimentation of nickel-based super alloys, solution heat treatment is more important than aging [4].
In solution heat treatment, the alloy is placed in a single phase containing the equilibrium diagram of phases for a period of time. Then it is quenched to create a supersaturated solid solution.
The important parameters are temperature, time, heating and cooling rates [1,2]. According to the mentioned issues, the purpose of this study is to investigate the microstructure of the IN718 nickel-based super alloy in various conditions of cooling after the solution heat treatment produced by SLM.
This research attempts to study the effect of the cooling rate in dissolution stage of different structures on the characteristics of primary and secondary precipitates. This research covers some aspects of the science, characterization, technology and application of environmental friendly materials.

2. Materials and Methods

Samples prepared by selective laser melting (SLM) from IN718 nickel-based super alloy were selected for this study. The chemical composition of IN718 obtained by the three-point test method in emission Spectrometry is shown in (Table. 1.).
Cube shaped samples were prepared in a 5 mm dimension for testing.
The schematic design and image of the samples prepared for analysis are shown in Fig. 1.
The prepared samples were imposed under the solution heat treatment within a tube furnace under the protective atmosphere of argon gas with purity of 99.99% at a temperature of 1040°C and 120 min of solubilization.
After completion of the solution, samples were quenched in three cold environment of water, air and open-door extinguished furnace. In Table. 2., solution conditions of various samples have been presented. After dissolution, samples were polished with SiC emery from the number 100 to 2500. Afterwards, they were polished by 6µm felt and 7% nano-alumina solution. For metallographic analysis, samples were immersed in a solution of 20ml HCl + 20ml C_2H_5OH + 2gr $CuCl_2$ for 15 minutes. Microstructural investigations were carried out using Optical Microscopes (OM) (Euromex-IScope-Netherland) and Field Emission Scanning Electron Microscopes in secondary electron mode with working voltage of 15kV (FESEM: MIRA2 VEGA, TESCAN, Czech Republic) equipped with spot analysis of EDS elements.
Fuzzy analyzes were performed by the X-ray diffraction (XRD) analysis (W1730 Philips) with wave length of 1.542 Å Cu Kα and scanning speed of 2 degree per minute and Export software.
Micro-hardness of samples was examined before and after solubilization by KOPA micro hardness tester (14460-Iran) at a load of 100 g and 10 seconds holding time according to ASTM E82 – 16.

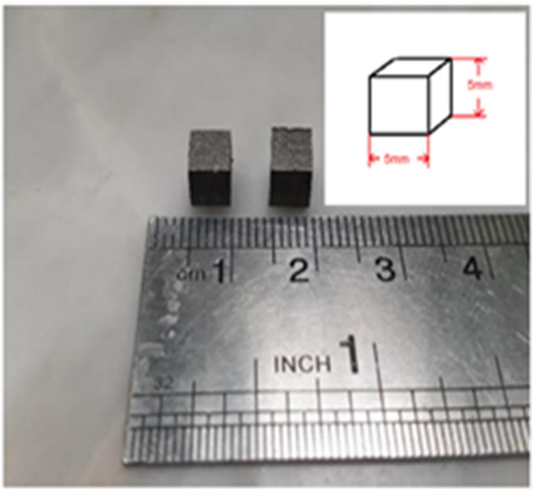

Fig. 1. Schematic design and sample image prepared.

Table. 2. Samples based on the cooling rate after solution treatment.

Samples	Solution			
	Temperature (°C)	Time (min)	Cooling Environment	Cooling Rate (°C/sec)
A0*	---	---	---	---
A1	1040	120	Water	255.000
A2	1040	120	Air	5.630
A3	1040	120	Furnace	0.094

*** Control Sample**

Table. 1. Chemical composition of super alloy (wt. %).

Ni	Si	Mn	Cr	Mo	Cu	Fe	Ti	Al	Nb	Co	P	S	C	B
Base	0.130	0.050	19.100	2.950	0.100	18.500	0.910	0.450	5.040	0.070	0.005	0.015	0.035	0.006

3. Results and Discussion

The image of samples produced by SLM method by optical microscopes (OM) and field emission scanning electron microscopes (FESEM) are shown in Fig. 2.

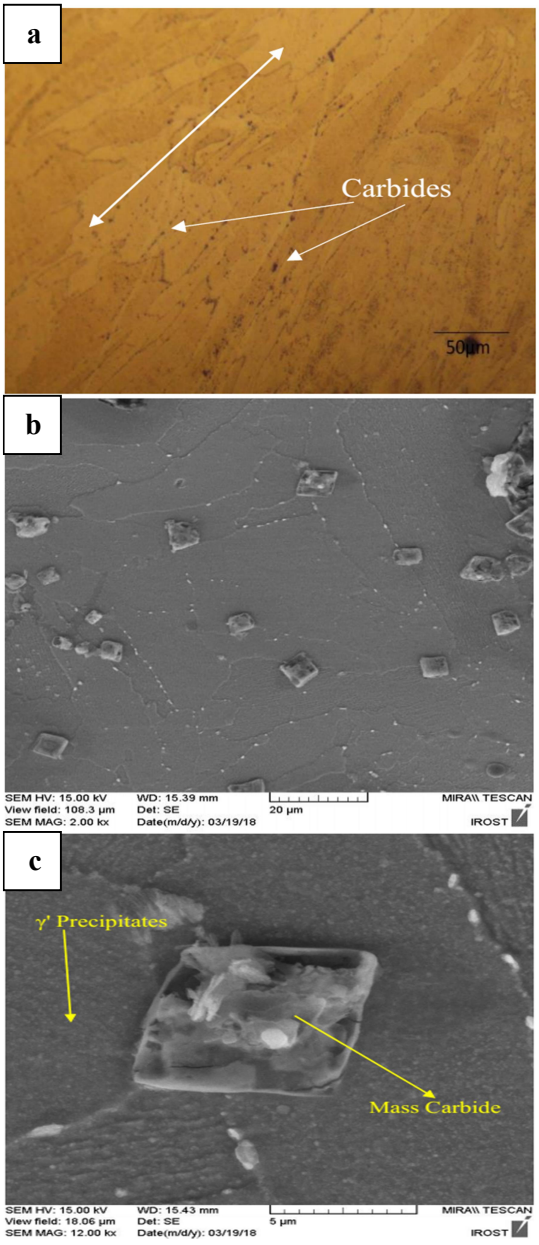

Fig. 2. a. Sample image by OM (SLM), (two-way arrow for grains' stretch); b. FESEM image, SLM reference sample containing MC initial carbides and orientation of grains, c. MC initial carbides and precipitates masses.

According to Fig. 2. and previous studies on the SLM sample, precipitates and carbides are very tiny due to the high freezing velocity during the production process.

These particles are not clearly visible, as well as the columnar drawn grains are seen in a direction (manufacture direction). Investigations on the SLM of the IN718 alloy show that strengthening phases are in the structure of γ″ [7-11].

Studies also show that in the SLM of the IN718 alloy, the amount of strengthening phases γ′ and γ″ produced in the matrix is very small due to the high temperature and fast freezing rate, while a large amount of carbide and a very fine lave phase can be found [12-16].Therefore, SLM of IN718 alloy has a much lower strength than after the heat treatment.

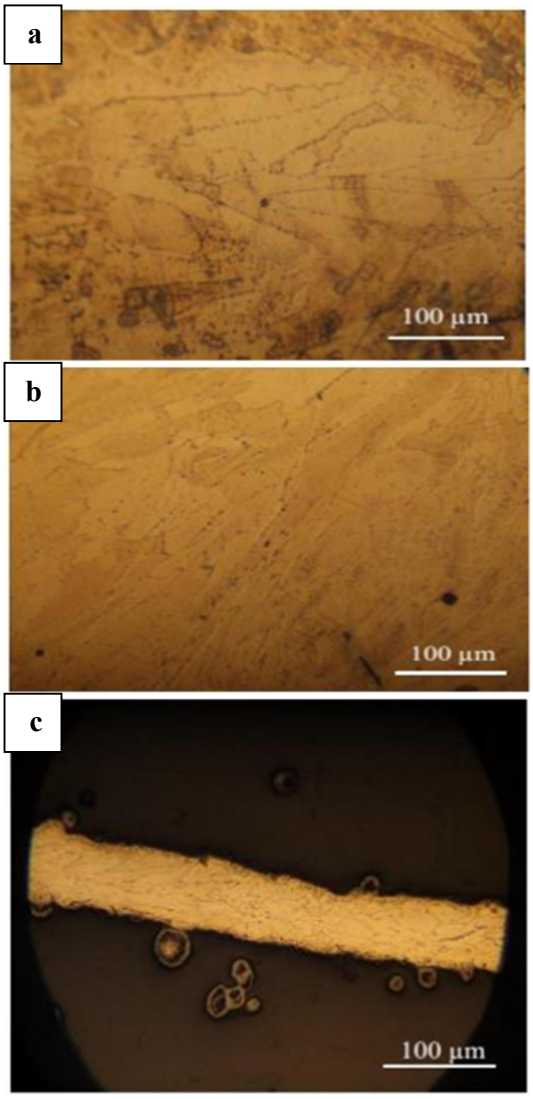

Fig. 3. Illustration of SLM samples after dissolution. a. cooled in water; b. cooled in air; and c. cooled in a furnace.

The heat treatment must be properly optimized in order to dissolve the lave phase and to stabilize the strengthening phases of γ′ and γ″, respectively, and also the formation of the δ phase is delayed [11, 13].

In order to remove Nb separation and improve mechanical properties, it is essential that the temperature of homogenization, solubility, or storage time of homogenization or solubility be greater. The IN718 texture in the SLM method can vary with the specific process parameters.

But the tissue is progressed parallel to construction [001] and the crystallographic directions are relatively isotropic.

In addition to the microstructural characteristics, the focus on construction directions is dependent on the mechanical properties of the structure [15-17].

According to previous research, the γ′′particles' dispersion points are in the direction of [100] and perpendicular to the main axis of the precipitates. Only the above network γ′′ has been appeared in the directions <100>, <½10>, and <1½0>. The masses of γ′′ are precipitated in parallel to construction formation. Precipitates of γ′′ with plates (100) are symmetrical, while in some cases they are corresponded to pages (010). Dense and often irregular accumulation with different geometries and very small sizes, precipitates γ′′ occurs throughout the field of γ NiCr (fcc) [7]. In Fig. 3., OM images of SLM Solutionized and cooled samples in different cooling environments is shown. In these images, a directional microstructure is observed in which the seeds have grown to produce a sample (SLM). In SLM process, the strengthening mechanism is the residual stress [18, 19]. It is in vain to expect that the cooling rate has a very small effect on the grain size. But dissolution due to high temperatures and high temperature-based intrusive mechanisms (due to higher temperatures than recrystallization) ruins the grain boundary, changes and increases the size of grains. Another mechanism that can be considered to increase the grain size is the movement of the grain boundaries to dissolve the blade phases and barrier carbides around the grain boundary during solubilization [7]. In Fig. 4., the graph of these changes is shown.

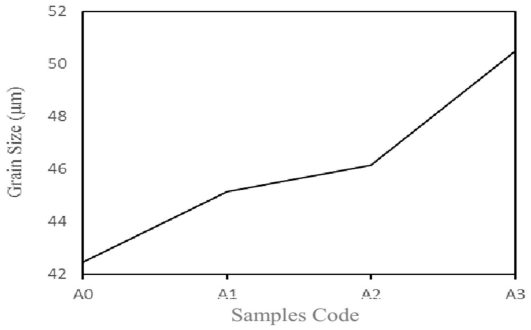

Fig. 4. Grain size variation of SLM sample due to the cooling rate.

As shown in Fig. 4., the cooling rate does not affect the grain size, and almost the samples cooled in water and air have grain size alike the reference sample.

But the sample cooled in the furnace had a noticeable change in size due to its long-term heat exposure. FESEM images of selective laser melting (SLM) samples in three cooling environments are shown in Fig. 5. also, Fig. 7. shows the image of the EDS analysis peak with points indicated by the yellow arrow in section (b) of Fig. 5.

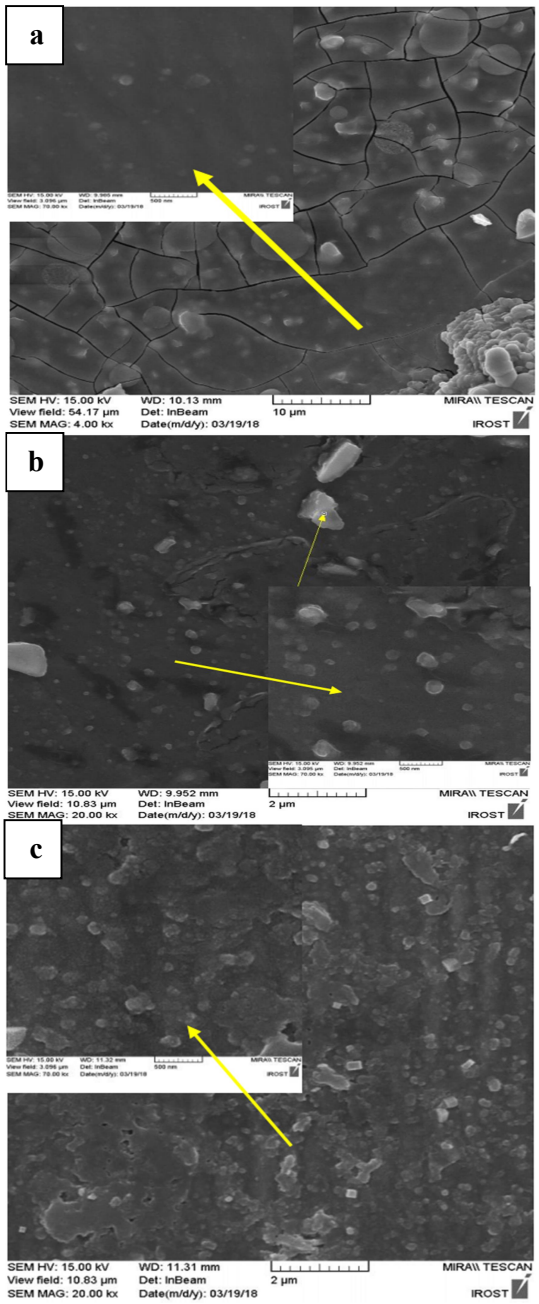

Fig. 5. FESEM image of SLM samples after solution, a) cooled in water, b) cooled in air, and c) cooled in a furnace.

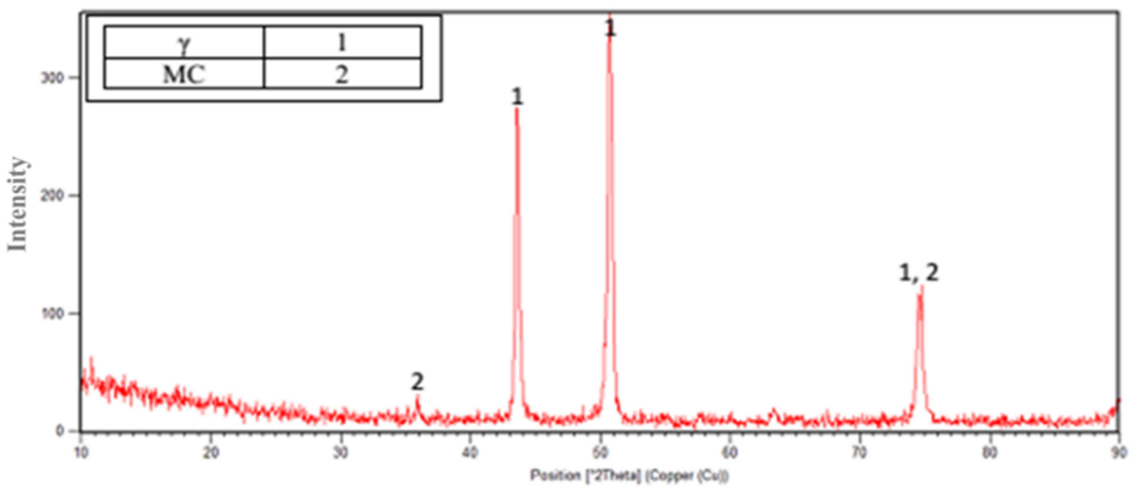

Fig. 6. The XRD model of SLM sample cooled in water.

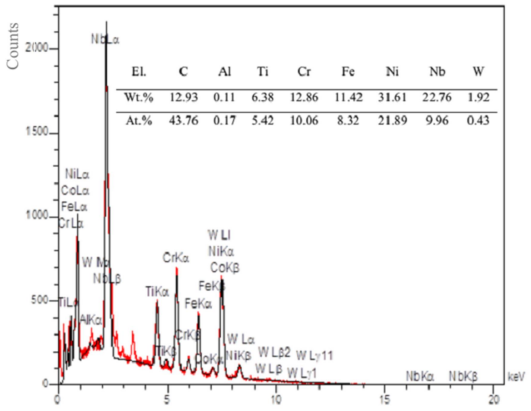

Fig. 7. Result of the EDS test of the indicated point which specified in section (b) of Fig. 5.

As shown in the Fig. 7., the specified point is the MC carbide and contains high values of Nb. The specified values of Ni, Fe and Cr are inserted from the adjacent points in the test results for identification by EDS. As shown in Fig. 5., the volume fraction of precipitates has been decreased after dissolution insofar in many parts of cooled points in water, there were no spherical precipitates of γ, pseudo spherical and elliptic precipitates of γ" and stretched precipitates of δ and these images were prepared after a large search of the considered sample. After cooling in water and specially in the furnace, e nanometer precipitates equilibrium cooled have opportunity to be formed and grown, which this issue is well illustrated in sections (b) and (c) of Fig. 5. In Fig. 6., an XRD image of SLM sample cooled in water after dissolution is illustrated.

This model confirms the complete solution. Precipitates appeared in part (A) of Fig. 5. were formed equilibrium and due to their very small volume fraction, peaks related to secondary precipitates have not been identified.

The micro hardness results of samples in the first solutionization step at 1040°C for 2 hours and cooling in three medium including water, air and furnace is shown in Fig. 8.

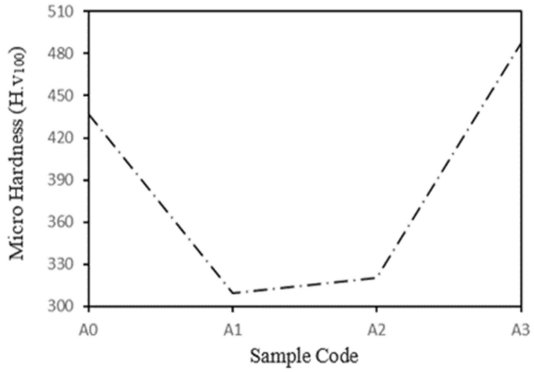

Fig. 8. Hardness changes after solutionizing and various cooling rate.

It can be concluded that increasing the cooling rate in the solution heat treatment step postpones nucleation of γ′ phase from matrix due to decrease of the atoms' mobility and consequently nucleation rate of γ′ phase increases while the growth is limited in the aging, and ultimately leads to an increase in preferential sites for nucleation of γ′′ phase and increase of the strength [20-23].

According to the SEM images and the results of micro hardness, it can be concluded that with decreasing the cooling rate in the solution heat treatment due to higher energy and the existence of more preferable sites for precipitates of γ′ phases, the higher hardness was obtained compared to the reference sample.

4. Conclusions

1. Present study can be considered as a start point for the heat treatment of nickel based superalloys produced by the SLM method.
2. During solutionizing heat treatment, grains size have increased and the cooling rate does not affect the grain size; Cooling in the furnace led to a significant increase of about 10 µm of grain size due to holding in high temperature.
3. The results of SEM and XRD showed that by solution heat treatment, at 1040°C and 2 hours and cooling in the water, the dissolution was completed and only a small amount of NbC carbide remained.
4. By decreasing in cooling rate of samples after dissolution, the size and volume fraction of secondary precipitates and carbides increased based on the equilibrium and cooling mechanisms.
5. Due to soltuionizing heat treatment, the hardness decreased because of dissolving of precipitates. Decreasing the cooling rate after dissolution led to increase the hardness due to the nucleation and growth of secondary precipitates in equilibrium or cooling mode.

References

[1] M. G. Oskouei : Gas Turbines, Ministry of Energy, Tehran, (2002), 73.
[2] L. A. Jackman : Forming, Fabrication and Heat Treatment of Superalloys, , in Superalloys Source Book, ASM, New York, (1984), 217.
[3] Y. Shajar and S. H. Razavi, 5th Int. Conf. of Materials and Metallurgy, iMat, Shiraz, (2016), 215.
[4] S. Bose and A. Bandyopadhyay : Additive Manufacturing, CRC Press, Boca Raton, Florida, CRC Press, (2016), 75.
[5] A. A. Antonysamy, , Ph.D. Thesis, University of Manchester, Manchester, (2012).
[6] B. Zhang, H. Liao, and C. Coddet, App. Surf. Sci., 279 (2013), 310.
[7] K. N. Amato, S. M. Gaytan, L. E. Murr, E. Martinez, P. W. Shindo, J. Hernandez, S. Collins, and F. Medina, Acta. Materialia. 60 (2012), 2229.
[8] J. P. Choi, G. H. Shin, S. Yang, D. Y. Yang, J. S. Lee, M. Brochu and J. H. Yu, Powder. Technol. 310 (2017), 60.
[9] J. Strößner, M. Terock and U. Glatzel. Adv. Eng Mater., 17 (2015), 1099.
[10] Q. Jia and D. Gu, J. Alloy. Compd., 585 (2014), 713.
[11] D. Zhang, W. Niu, X. Cao, and Z. Liu, Mater. Sci. Eng. A., 644 (2015), 32.
[12] T. Trosch, J. Strößner, R. Völkl, and U. Glatzel, Mater. Letters., 164 (2016), 428.
[13] E. Chlebus, K. Gruber, B. Kuźnicka, J. Kurzac, and T. Kurzynowski, Mater. Sci. Eng. A., 639 (2015), 647.
[14] M. E. Aydinöz, F. Brenne, M. Schaper, C. Schaak, W. Tillmann, J. Nellesen, and T. Niendorf, Mater. Sci. Eng., 669 (2016), 246.
[15] Z. Wang, K. Guan, M. Gao, X. Li, X. Chen, and X. Zeng, J. Alloy. Compd. 513 (2012), 518.
[16] D. H. Smith, J. Bicknell, L. Jorgensen, B. M. Patterson, N. L. Cordes, I. Tsukrov, and M. Knezevic, Mater. Character., 113 (2016), pp. 1.
[17] Y. L. Kuo, S. Horikawa, and K. Kakehi, Mater. Design., 116 (2017), 411.
[18] M. F. Zaeh and G. Branner, Production. Eng., 4 (2010), 35.
[19] P. Mercelis and J. P. Kruth. Rapid. Prototyping. J. 12 (2006), 254.
[20] M. P. Jackson, M. J. Starink, and R. C. Reed, Mater. Sci. Eng. A., 264 (1999) 26.
[21] E.H. Vander Molen, Metal. Trans., 2 (1971) 1627.
[22] Z. Baicheng, L. Xiaohua, B. Jiaming, G. Junfeng, W. Pan, S. Chen-nan, N. Muiling, Q. Guojun and W. Jun, Mater. Design., 116 (2017), 531.
[23] P.E. Mosser, Proc. Of 6th Int. Symp. In Metallurgy of Superalloys, Pennsylvania, (1989), 179.